SODIUM CURRENT IN VOLTAGE CLAMPED INTERNALLY PERFUSED CANINE CARDIAC PURKINJE CELLS

JONATHAN C. MAKIELSKI, MICHAEL F. SHEETS, DOROTHY A. HANCK, CRAIG T. JANUARY, AND HARRY A. FOZZARD

The Cardiac Electrophysiology Laboratories, Departments of Medicine and the Pharmacological and Physiological Sciences, The University of Chicago Pritzker School of Medicine, Chicago, Illinois 60637

ABSTRACT Study of the excitatory sodium current (I_{Na}) in intact heart muscle has been hampered by the limitations of voltage clamp methods in multicellular preparations that result from the presence of large series resistance and from extracellular ion accumulation and depletion. To minimize these problems we voltage clamped and internally perfused freshly isolated canine cardiac Purkinje cells using a large bore (25-μm diam) double-barreled flow-through glass suction pipette. Control of $[Na^+]_i$ was demonstrated by the agreement of measured I_{Na} reversal potentials with the predictions of the Nernst relation. Series resistance measured by an independent microelectrode was comparable to values obtained in voltage clamp studies of squid axons (<3.0 Ω-cm^2). The rapid capacity transient decays ($\tau_c < 15$ μs) and small deviations of membrane potential (<4 mV at peak I_{Na}) achieved in these experiments represent good conditions for the study of I_{Na}. We studied I_{Na} in 26 cells (temperature range 13°–24°C) with 120 or 45 mM $[Na^+]_o$ and 15 mM $[Na^+]_i$. Time to peak I_{Na} at 18°C ranged from 1.0 ms (−40 mV) to less than 250 μs (+40 mV), and I_{Na} decayed with a time course best described by two time constants in the voltage range −60 to −10 mV. Normalized peak I_{Na} in eight cells at 18°C was 2.0 ± 0.2 mA/cm^2 with $[Na^+]_o$ 45 mM and 4.1 ± 0.6 mA/cm^2 with $[Na^+]_o$ 120 mM. These large peak current measurements require a high density of Na^+ channels. It is estimated that 67 ± 6 channels/μm^2 are open at peak I_{Na}, and from integrated I_{Na} as many as 260 Na^+ channels/μm^2 are available for opening in canine cardiac Purkinje cells.

INTRODUCTION

Difficulties in voltage clamping the excitatory sodium current (I_{Na}) in heart muscle have been well described (Johnson and Lieberman, 1971; Fozzard and Beeler, 1975; Beeler and McGuigan, 1978). The best efforts to circumvent these difficulties in multicellular preparations have been those of Colatsky (1980), who used short Purkinje strands from rabbit, and those of Ebihara et al. (1980), who used small aggregates of embryonic chick heart cells. Those studies suggested that cardiac I_{Na} generally resembled I_{Na} in the squid giant axon (Hodgkin and Huxley, 1952), but they may not have had sufficient membrane voltage control to determine kinetic details. Recently, single cell clamp and patch clamp have improved the study of I_{Na} in cardiac cells. I_{Na} in single mammalian cardiac cells has been studied by voltage clamp (Brown et al., 1981; Bustamante and McDonald 1983; Bodewei et al., 1982; and Benndorf et al., 1985) and single Na^+ channel current in cardiac tissue has been studied by patch clamp (e.g., Cachelin et al., 1983; Grant et al., 1983; Patlak and Ortiz, 1985; Kunze et al., 1985). Patch clamping provides details of I_{Na} kinetics revealed by single channel openings and closings that are not available from whole cell recordings. However, single channel studies are not a substitute for whole cell studies because they are more limited by a low signal-to-noise ratio, which restricts study to certain voltage ranges, ion concentrations, and frequency ranges, and by longer capacity transients that may influence or obscure events that closely follow voltage clamp step changes.

We have adapted the technique of whole cell voltage clamp using a large flow-through glass suction pipette to study I_{Na} in freshly dissociated canine cardiac Purkinje cells. A single large suction pipette allows for rapid control of intracellular Na^+ ($[Na^+]_i$) and K^+ concentrations (Kostyuk, 1984), and for decreased series resistance (R_s) compared with smaller suction pipettes (Brown et al., 1981). The canine cardiac Purkinje cell should also have advantages over other cardiac cells for voltage clamping because its larger diameter and lack of t-tubules (Sommer and Johnson, 1979; Mathias et al., 1985) result in a smaller R_s.

It is also important to study I_{Na} in cardiac muscle because studies of non-cardiac I_{Na} may not apply to cardiac I_{Na}. Cardiac I_{Na} differs from I_{Na} in other tissues in its sensitivity to tetrodotoxin (Brown et al., 1981) and to saxotoxin (Rogart, 1981), and in its sensitivity to heavy

Address for correspondence to Dr. Jonathan C. Makielski, Section of Cardiology, Box 249, The University of Chicago, 5841 S. Maryland Ave., Chicago, IL 60637.

metal divalent ions (Frelin et al., 1986). The study of Purkinje cell I_{Na} in particular is important to cardiac electrophysiology because it allows correlation with previous studies of excitation and conduction in Purkinje fibers.

We show that our experimental technique achieves membrane potential control sufficient to compare I_{Na} in Purkinje cells with that in other tissues such as the squid axon and that it controls $[Na^+]_i$. Comparison of our results with previous measurements in heart shows that the onset of I_{Na} is more rapid, the decay of I_{Na} is better described by a two exponential process (as also described by Brown et al., 1981; Patlak and Ortiz, 1985; and Kunze et al., 1985), and the current density measured in these experiments exceeds previously published reports in heart by one or two orders of magnitude.

METHODS

Preparation of Cells

The method for preparing single canine cardiac Purkinje cells has been described in detail elsewhere (Sheets et al., 1983). Briefly, canine Purkinje fibers from the hearts of adult mongrel dogs were cut in short segments (2–3 mm) and placed in Eagle's minimal essential medium modified to contain 0.1 mM free Ca^{++} (by the addition of EGTA), 5.6 mM Mg^{++}, 5.0 mM HEPES, 1 mg/ml albumin, and 5 mg/ml Worthington type I collagenase buffered to pH 6.2. The fibers were incubated in this digestion solution at 37°C, gassed with 100% O_2, and gently agitated for 3–4 h. After a brief incubation in 130 mM K-glutamate, 5.7 mM Mg^{++}, 0.1 mM EGTA, 5.0 mM glucose, and 5.0 mM HEPES (pH 6.2), the cells were mechanically dispersed and were maintained in Eagle's minimal essential medium with 1.0 mg/ml albumin (pH 7.2) at room temperature. They were studied within 12 h of isolation.

All solutions were made from reagent grade chemicals and were filtered through 0.22-μm Millipore filters. Standard extracellular solutions contained 45 mM Na^+, 105 mM Cs^+, 1.0 mM Mg^{++}, 3.0 mM Ca^{++}, 154 mM Cl^-, 10.0 mM HEPES, and 5.5 mM glucose at pH 7.2. Standard intracellular solutions contained 15 mM Na^+, 134 mM Cs^+, 134 mM F^-, 15 mM $H_2PO_4^-$, 10.0 mM HEPES, 5.0 mM EGTA, 5.0 mM glucose, 0.1 mM Mg-ATP, and 0.1 mM 8-Br cAMP at pH 7.2. Solutions with different Na^+ concentrations were made by substituting Na^+ for Cs^+ while keeping the ionic strength the same.

Suction Pipettes

Fig. 1 shows a schematic of the suction pipette used in this study. 2 mm outside diameter borosilicate theta glass (R&D Scientific Glass, Spencerville, MD) with the septum partially removed was pulled on a Narishige (Tokyo, Japan) microelectrode puller. The tip was fractured with a diamond-tipped pencil and fire-polished to give pores with diameters of 20–30 μm. Flow of intracellular solutions through the pipette was adjusted by moving a hydrostatic column attached to the outlet (approximate flow 1 ml/min). Resistance of the pipettes in standard solutions without a cell attached was ~50 kΩ. Mean total resistance in standard solutions with the cell attached was 42 ± 6 MΩ (±SE, n = 22). Assuming that the resistance represents the seal of cell membrane to glass, the seal resistance was 3.2 GΩ per micrometer of pipette–cell contact. The actual seal resistance will be greater than this value depending upon the contribution of the cell membrane to total resistance. Membrane resistance in the absence of K^+, however, is likely to be high (≥100 MΩ) so that total resistance should provide a good estimate for the quality of the seal.

Standard glass microelectrodes (1.0-mm OD, WPI) were pulled using a Brown-Flaming puller (Sutter Instruments, San Rafael, CA) and filled with 3.0 M KCl.

Experimental Procedures

Studies were conducted at room temperature, which was varied between 13° and 24°C. The preparation, experimental apparatus, and both the pipette and bath solutions were allowed to equilibrate with room temperature for at least 1 h before studies were performed. Cells were transferred to the experimental chamber and drawn into the pipette pore by application of negative pressure and allowed to seal to the glass leaving only a part of the cell extending into the bath (Fig. 1). The part of the cell inside the pipette was disrupted by a 25-μm diam platinum wire advanced down the outflow barrel of the pipette. After sealing, cells remained viable on the pipette tip commonly for 1 h and occasionally for up to 4 h. Electrophysiological measurements reported here, however, were completed as soon as possible after disruption because kinetic parameters (activation and inactivation) shifted with time on the voltage axis in a negative direction (Fozzard et al., 1986, and Fig. 9). The only experimental results to be included in the analysis are those for which post-control measurements differed minimally from pre-control measurements. Voltage protocols and/or solution changes were designed to allow for such controls.

Electronic Apparatus

Voltage control was imposed through a summing junction to a unity gain operational amplifier (model OPA27; Burr-Brown Corp., Tucson, AZ)

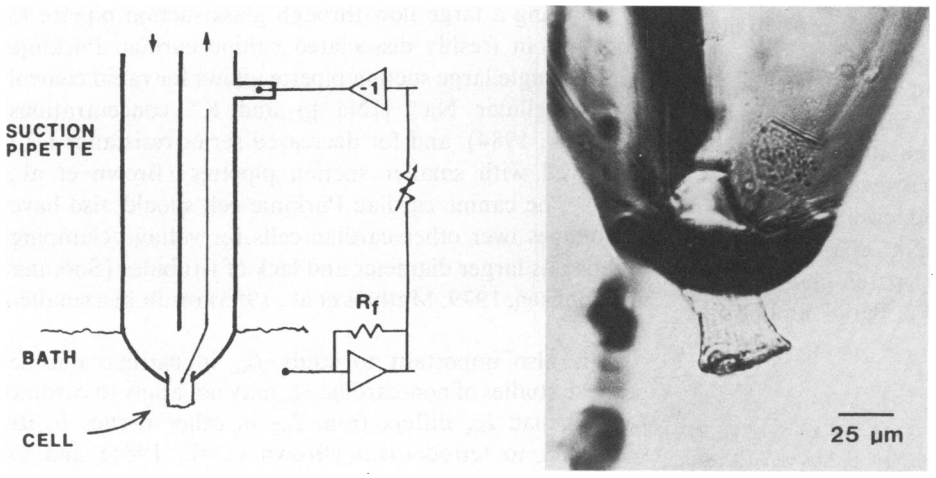

FIGURE 1 (*Left*) Diagram of perfusion pipette and electronics. (*Right*) Photograph of a single Purkinje cell in the perfusion pipette. See text for details

connected to the pipette solution through a Ag/AgCl pellet (E.M. Wright, Guilford, NC) and a 3 M KCl agar bridge. Current was measured by a current to voltage amplifier (model OPA102 or OPA101; Burr-Brown Corp.) connected to the bath through a second 3 M KCl agar bridge and Ag/AgCl pellet. A portion of the measured current could be fed back to compensate for R_s of the pipette and preparation. In the absence of a cell the response of this circuit to the largest step change in voltage imposed experimentally (250 mV) was 99% complete within 10 μs. Junction potentials, measured by connecting the intracellular solution with the extracellular solution through a 3 M KCl agar bridge, were found to be <0.6 mV and were neglected. Standard glass microelectrodes were connected through Ag/AgCl pellets to an electrometer (model 750; W-P Instruments, Inc., New Haven, CT).

Voltage Clamp Protocols, Data Acquisition, and Analysis

Command voltage steps were generated by a 12-bit D/A converter and currents were recorded at either 100 or 300 kHz by a 12-bit A/D converter both of which were controlled by a Masscomp 5500S microcomputer (Westford, MA). The inherent bandwidth of the system provided adequate filtering for signal acquisition at 300 kHz. In later records signals recorded at 100 kHz were prefiltered at a cutoff frequency of 50 kHz (8-pole Bessel filter, Frequency Devices, Inc., Haverhill, MA).

Data were analyzed on the Masscomp 5500S computer. The capacity transient (I_{cap}) was recorded at 300 kHz and average traces were constructed from the absolute value of the current responses to four hyperpolarizing voltage steps from −150 to −190 mV and four depolarizing voltage clamp steps from −190 to −150 mV. Membrane capacitance (C_m) was measured by integrating the average transient for 1 ms, although estimates of C_m were constant by 100 μs. I_{Na} was recorded at 100 kHz and records were digitally filtered (Gaussian) at 5 kHz before analysis. I_{Na} measurements were normalized to C_m and then to membrane surface area by assuming a C_m of 1 μF/cm^2. Current decays were analyzed as a sum of exponentials by a Fourier method (Provencher, 1976) that determined the number, amplitudes, and time constants of the components. Summary data are expressed as means (± SE) from up to 26 different cells.

Identification of I_{Na}

The transient current appearing on depolarization, reversing at the Na reversal potential calculated by the Nernst relation, and sensitive to tetrodotoxin (TTX) was identified as I_{Na}. I_{Na} amplitudes were measured by subtracting the current remaining at the end of the 25-ms clamp step from the peak transient current. The current–voltage relations at the end of 25-ms clamp steps showed small inward current deviations from linearity between −60 and 0 mV, which were blocked by TTX and probably represented residual I_{Na}. Occasionally a delayed outward current (<1–2% of peak I_{Na}) developed at step potentials positive to +40 mV, which probably represented a nonspecific outward current that has also been noted in nerve (Brown et al., 1980).

RESULTS

Control of the Electrical and Chemical Gradients

Membrane voltage with R_s compensation was directly measured during peak I_{Na} by a fine-tipped glass micropipette impaled into the distal end of the cell. A representative trace during a voltage clamp step to −40 mV from a holding potential of −150 mV is shown in Fig. 2. The deviation from command potential during peak I_{Na} of 92 nA was <4 mV at the distal end of the cell, giving an R_s of 43 KΩ. Normalizing to C_m (67 pF) gives an R_s of 2.9 Ω-cm^2. In this cell the peak current was reduced to 80 nA when R_s compensation was removed, and the voltage deviation at peak I_{Na} was 10 mV, giving an R_s of 125 kΩ (8.4 Ω-cm^2). Working in reduced Na^+ gradients, lowering the experimental temperature, and studying only a portion of the cell membrane helped control membrane voltage during peak I_{Na}.

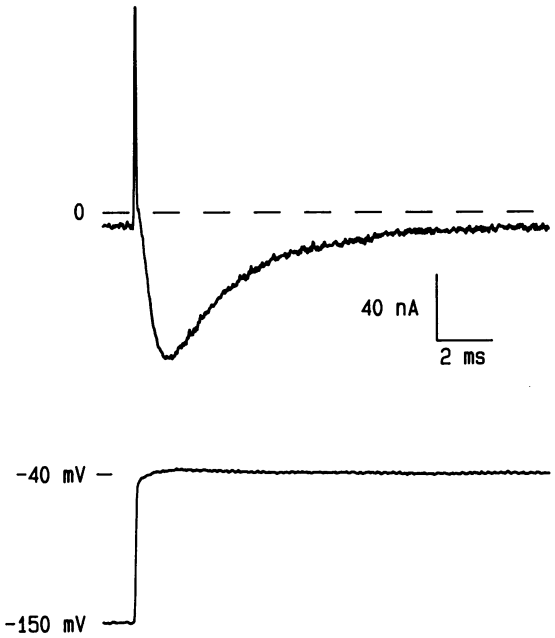

FIGURE 2 Independent measure of voltage control. Current response to a depolarization from −150 to −40 mV imposed through the suction pipette. The capacity transient was not faithfully reproduced because the peak was off scale and the current record was filtered at 5 kHz. (Cell 28.03, 120 mM $[Na^+]_o$, 15 mM $[Na^+]_i$, Temp. 15°C, C_m = 67 pF.) The current trace was partially corrected for periodic noise by background subtraction. Membrane potential was measured by a capacity compensated conventional glass microelectrode impaled into the distal end of the cell. The microelectrode response followed membrane potential during I_{Na} and shows a maximum deviation from the command potential of <4 mV.

The capacity transient was analyzed in each cell to help assess adequacy of access to the cell interior for voltage clamp. I_{cap} records from a representative cell with and without R_s compensation are shown in Fig. 3. After vigorous disruption of the cell segment inside the pipette, the decay of I_{cap} approximated a single exponential with a decay time constant (τ_c) < 15 μs. Inadequate disruption of the cell segment resulted in decay of I_{cap} that was clearly bi-exponential. In the present study only those experiments in which I_{cap} demonstrated good disruption were included for analysis. Capacitance of the cell segment was calculated from the area under the transients and the mean C_m for 17 cells was 74 ± 5.8 pF.

Control of intracellular and extracellular $[Na^+]$ was demonstrated by measuring reversal potential (E_{rev}) with

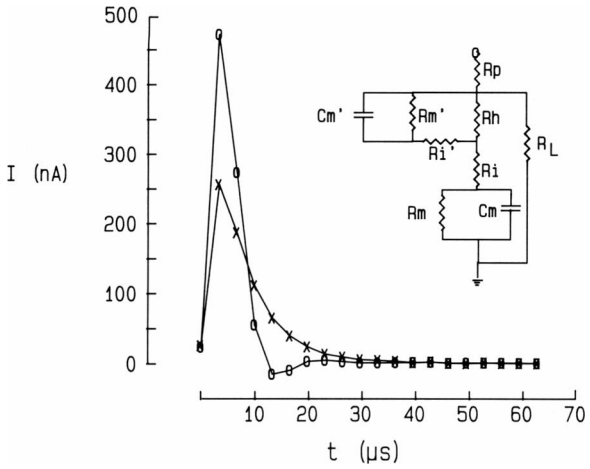

FIGURE 3 Capacity current records (see Methods) with (0) and without (×) R_s compensation. (Cell 13.02, Temp. 18°C, sampled at 300 kHz.) (*Inset*) Equivalent circuit proposed for the cell preparation to explain the presence of two components of exponential decay in the capacity transient and the effects of making the access hole larger. R_p, pipette resistance; R_h, resistance of the hole in the cell; R_L, resistance of the paracellular leak; R_i and R'_i, intracellular resistances; C_m and C'_m, membrane capacitance; R_m and R'_m, membrane resistance. C'_m, R'_m and R'_i refer to the part of the cell inside the pipette, and C_m, R_m, and R_i refer to the cell outside the pipette.

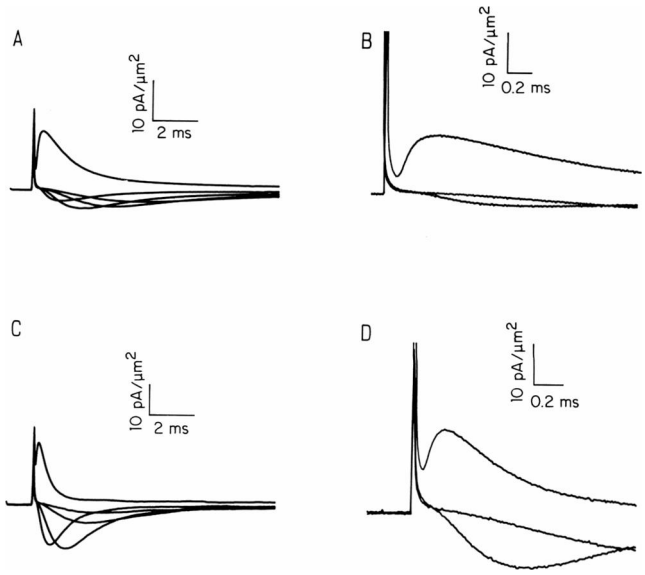

FIGURE 4 Raw digitized current records (no leak or capacity correction) for two cells in response to step depolarizations from −150 mV. In *A* steps were to −55, −50, −40, −20, and +80 mV; in *B* steps were to −50, −20, and +80 mV; in *C* steps were to −60, −50, −40, −20, and +100 mV; in *D* steps were to −50, −20, and +100 mV. The panels on the right show the early time course of currents. Note the separation of the capacity transient from I_{Na} and the sigmoid turn-on of I_{Na}. (*A* and *B*) From cell 44.01 in 45 mM $[Na^+]_o$ and 45 mM $[Na^+]_i$ at 12°C with 8-pole Bessel filter at 50 kHz before A/D sampling at 100 kHz; (*C* and *D*) from cell 17.03 in 45 mM $[Na^+]_o$ and 15 mM $[Na^+]_i$ at 17°C without filtering before A/D sampling. *A* and *C* were digitally filtered at 5 kHz and the capacity spike is attenuated; *B* and *D* were not digitally filtered.

different $[Na^+]_i$ and $[Na^+]_o$ in the perfusate solutions. Stable E_{rev} was achieved within 2 min for changes of intracellular solutions and within 30 s for changes of external solutions. Results from 19 cells showed close agreement (to within 1 mV) of the E_{rev} predicted by the Nernst relation with the experimental E_{rev} and indicated good perfusion of both intracellular and extracellular spaces (Table I).

Characteristics of I_{Na}

Current responses in two representative cells to a series of step depolarizations from a holding potential of −150 mV are shown in Fig. 4. In all experiments I_{Na} peaked earlier with more positive depolarizations and clear separation of peak I_{Na} from I_{cap} was achieved, even for strong depolarizations. This made it possible to make peak I_{Na} measurements without I_{cap} subtraction because differences between measurements with and without subtraction were <1 nA. Also note that inward I_{Na} activated with a sigmoid time course.

TABLE I
I_{Na} REVERSAL POTENTIALS

$[Na^+]_o/[Na^+]_i$	No. cells	n	Pred E_{rev}	Mean E_{rev}	SD
mM			*mV*	*mV*	*mV*
120:15	6	12	52	52	2
45:15	19	76	28	28	4
45:30	2	7	10	11	1
45:45	8	14	0	1	2
15:45	2	2	−27	−27	2
15:120	2	2	−51	−52	1

n, number of observations. Pred E_{rev}, reversal potential for I_{Na} predicted by the Nernst equation using perfusate concentrations $[Na^+]_o$ and $[Na^+]_i$. Mean E_{rev}, mean reversal potential, for I_{Na} as measured from the peak current voltage plot. SD, standard deviation.

I_{Na} decayed exponentially with a time course best described by more than one time constant in all cells analyzed for decays. During 25-ms depolarizations, I_{Na} decay was best fit by two time constants (τ_{h1} and τ_{h2}) over a wide voltage range and from holding potentials of −150 and −100 mV. Results from a typical cell are shown in Fig. 5. Both τ_{h1} and τ_{h2} were voltage dependent, decreasing steeply between −60 and −10 mV (n = 12 cells). Although two time constants of I_{Na} decay can be produced artifactually by poor voltage control, that is unlikely because τ_{h1} and τ_{h2} were unchanged even when I_{Na} magnitude was reduced by 55% by changing holding potential from −150 to −100 mV (n = 3 cells).

Fig. 6 shows fractional Na^+ channel availability assessed after conditioning prepulses to different potentials and normalized conductance estimated from step depolarizations in a typical cell. The best fit of the Hodgkin–Huxley (1952) model with m^3h kinetics is shown for comparison with the experimental data. The small overlap is consistent with our observation that a small fraction of I_{Na} (<2% of peak) persists at the end of 25 ms for

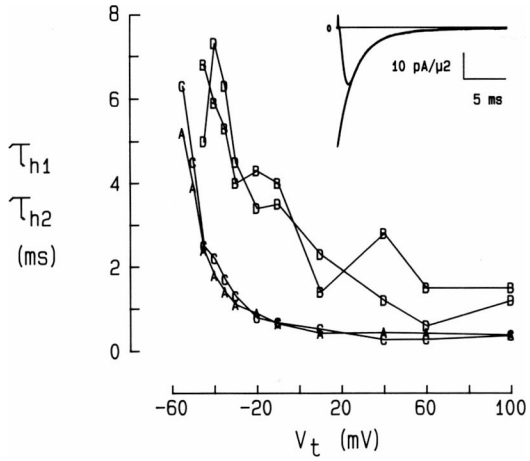

FIGURE 5 Dependence of I_{Na} decay on membrane potential with different I_{Na} magnitudes. Symbols represent fast time constant (τ_{h1}) at V_h −150 mV (*A*), slow time constant (τ_{h2}) at V_h −150 mV (*B*), τ_{h1} at −100 mV (*C*), τ_{h2} at −100 mV (*D*). Inset shows the exponential fit on the data for a depolarization to −40 mV from a holding potential of −150 mV. (Cell 13.02 45 mM $[Na^+]_o$, 15 mM $[Na^+]_i$ at 18°C.)

depolarizations between threshold and 0 mV, but it should be emphasized that our inability to resolve currents <1 nA in these studies limits investigation of this small steady or slowly decaying current. The discrepancy of the experimental data from the line describing a Boltzmann distribution between two states in the voltage range −90 to −120 mV was consistently observed and indicates that kinetics are more complex than the Hodgkin–Huxley model (e.g., see Chiu 1977; Fozzard et al., 1986). The hyperpolarizing shift in gating kinetics apparent in this figure is discussed below.

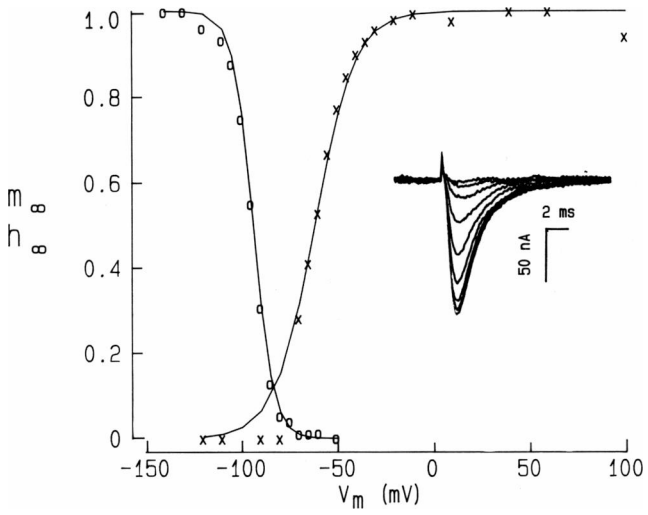

FIGURE 6 I_{Na} availability in response to step depolarizations to −20 mV after a 500-ms conditioning pulse to variable V_m (0). Activation values (×) were obtained by taking the cube root of normalized peak conductance values in response to a step depolarization to V_m from a holding potential of −150 mV. The solid lines are fits to the equation $1/\{1 + \exp[(V_m - V_{1/2})/\text{slope}]\}$ where for (0) the slope = 5.1 and $V_{1/2}$ = −94, and for (×) the slope = −10.5 and $V_{1/2}$ = −62. The inset shows current traces used to determine (0). (Cell 13.02, 45 mM $[Na^+]_o$, 15 mM $[Na^+]_i$, 18°C., V_h = −150 mV.)

Peak Current–Voltage Relationship

I_{Na} responses in a typical cell at 18°C to depolarizations from a holding potential of −150 or −100 mV are shown in Fig. 7, *A* and *B*, respectively, and their peak current–voltage (IV) relationships are shown in Fig. 7 *C*. Peak IV relationships with 15 mM $[Na^+]_i$ and either 45 or 120 mM $[Na^+]_o$ are shown in Fig. 7 *D*. I_{cap} is not well shown in the current traces because the first 20 μs after membrane depolarization were not plotted. The peak currents in Fig. 7 *C* resulting from a holding potential of −100 mV scale by a constant factor (2.22) to the peak currents from a holding potential of −150 mV.

All peak IV relationships demonstrated a graded response in the suprathreshold region and showed a maximum inward current at ~−40 mV. The maximum I_{Na} measured in eight cells studied in 45 mM $[Na^+]_o$ and 15 mM $[Na^+]_i$ at 18°–19°C was 19.1 ± 1.9 pA/μm². Slope conductance (G_{Na}) calculated from the positive slope of the peak IV relationship was 361 ± 28 pS/μm², and peak permeability (P_{Na}) calculated from the Goldman–Hodgkin–Katz (Hodgkin and Katz, 1949) constant field equation (GHK) was 32 ± 3.2 × 10^{-5} cm/s. In 10 cells studied in 120 mM $[Na^+]_o$ and 15 mM $[Na^+]_i$ at 18°–19°C maximum I_{Na} was 41.0 ± 5.4 pA/μm² and G_{Na} was 523 ± 75 pS/μm².

Temperature Effects on I_{Na}

22 cells were studied in 45 mM $[Na^+]_o$ and 15 mM $[Na^+]_i$ at temperatures of 13°–25°C. At 18°C I_{Na} peaked at 1.0 ms for a depolarization to −40 mV and at 250 μs to +40 mV. G_{Na} (Fig. 8 *A*) increased by a factor of nearly three over this temperature range, while the time to peak I_{Na} at −40 mV changed by a factor of about two (Fig. 8 *B*). Peak I_{Na} depends upon activation, inactivation, and open channel conductance in a complex manner; it should not be taken as an index of open channel conductance, which usually has a Q_{10} of 1.2–1.4 (e.g., Nagy et al., 1983). Nor can time to peak be considered an exact index of activation, which has a Q_{10} of 3.0 (Hodgkin and Huxley, 1952). Because previous studies of cardiac I_{Na} do not report a large number of experiments, we are uncertain whether the variability in G_{Na} from cell to cell relates to the tissue or to our experimental method. Attempts to correlate this variability with cell size, indices of voltage control, leak resistance, and temperature were unsuccessful.

Hyperpolarizing Shift in Kinetic Parameters

We have previously reported a shift in inactivation parameters in the internally perfused Purkinje cell (Fozzard et al., 1986). Immediately after access to the cell's interior,

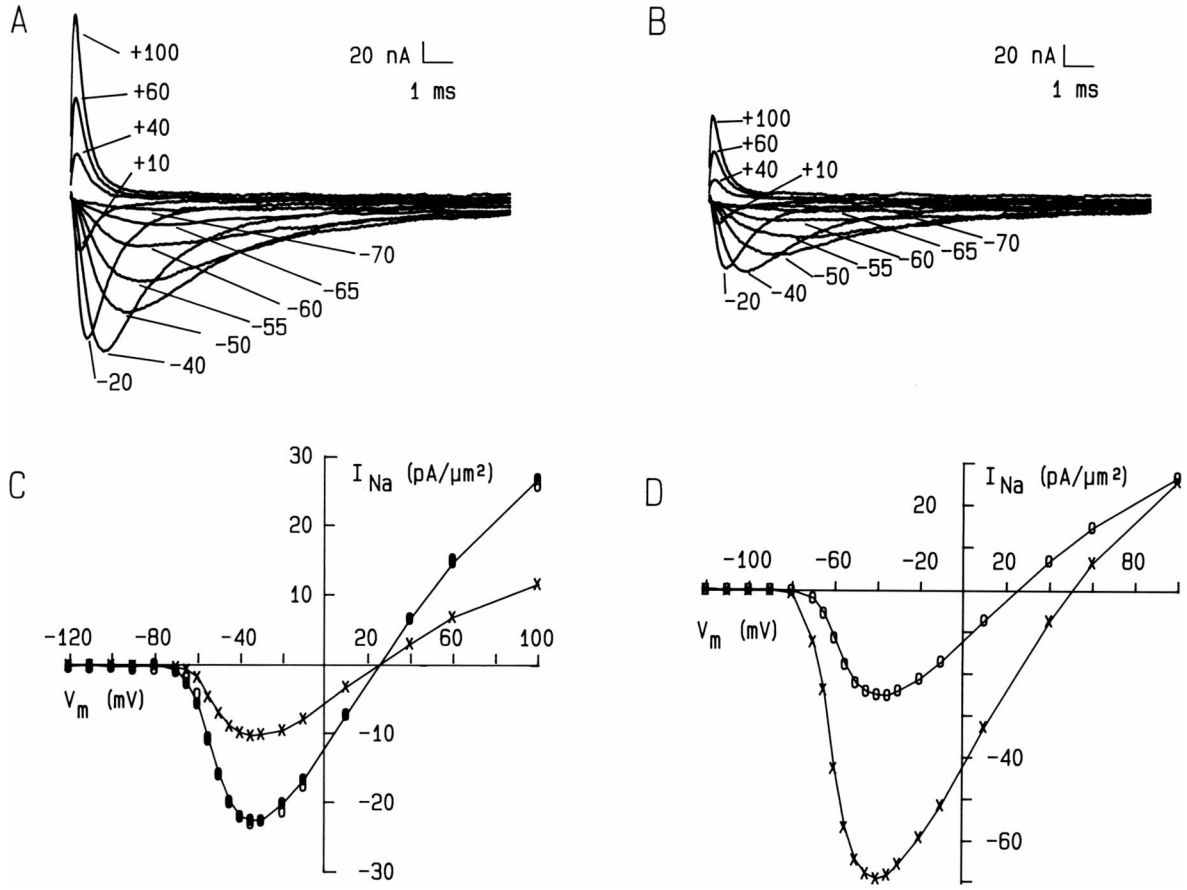

FIGURE 7 I_{Na} traces and peak IV plots from different holding potentials (V_h) with different Na gradients in the same cell. (*A*) Family of current traces in response to depolarizations from $V_h = -150$ mV, 45 mM $[Na^+]_o$, 15 mM $[Na^+]_i$. (*B*) As in *A* except $V_h = -100$ mV. (*C*) Peak IV plots of currents shown in *A* (filled circles, $V_h -150$ mV) and in *B* (*X*, $V_h -100$ mV). Open circles are the values of I_{Na} from $V_h -100$ mV (×) multiplied by a scaling factor of 2.22 to show scaling of the peak IV plot with differing I_{Na} magnitudes. (*D*) Peak IV plots in the same cell (current traces not shown) with $[Na^+]_o$ of 45 mM and 120 mM, $[Na^+]_i$ = 15 mM. (Cell 13.02, Temp. 18°C, filtered at 5 kHz.) Slope conductance increased from 446 pS/μm^2 to 835 pS/μm^2. P_{Na} was 41 × 10^{-5} cm/s and 39 × 10^{-5} cm/s.

the midpoint of the Na^+ channel availability curve was −90 mV. Although the midpoint continued to shift to more negative potentials for the duration of the experiment (Fig. 9), the rate of shift was sufficiently slow to allow completion of clamp protocols and solution changes with post-controls that were not significantly different from pre-controls. The shape of the Na^+ channel availability curve relation did not change with time but threshold potential and voltage at peak I_{Na} shifted to more negative potentials. Adding intracellular ATP or 8-bromo cAMP, lowering experimental temperature, or changing $[Ca^{2+}]_o$ did not stop the shift in I_{Na} kinetics.

DISCUSSION

We have described a technique that allows for the successful study of I_{Na} in single canine cardiac Purkinje cells. The striking differences between our results and those previously reported from other heart preparations are a greatly increased I_{Na} density and a more rapid onset and decay of I_{Na}. A comparison of I_{Na} from this study and those from other studies in single heart cells is presented in Table II.

I_{Na} measurement depends upon many factors such as uniformity of voltage control, normalization procedure, permeant and nonpermeant ion concentrations, and temperature, which differed in the studies cited in Table II. These factors must be considered before concluding that Na^+ channel properties are different in canine cardiac Purkinje cells than in ventricular or atrial cells.

Voltage Control

Membrane voltage control during peak I_{Na} is difficult in a cardiac cell because the size and speed of this current exceeds all other membrane currents, but good voltage control is essential to study I_{Na} magnitude and kinetics. We have shown good membrane voltage control during peak I_{Na} by direct measurement with a glass microelectrode impaled at the distal end of the cell and found the R_s to be <3 Ω-cm^2. This value compares favorably with that of the squid axon (Cole and Moore, 1960) and represents a significant improvement in R_s when compared with previous studies in heart (Table II). The improvements in R_s noted in this study are likely the result of the large size of

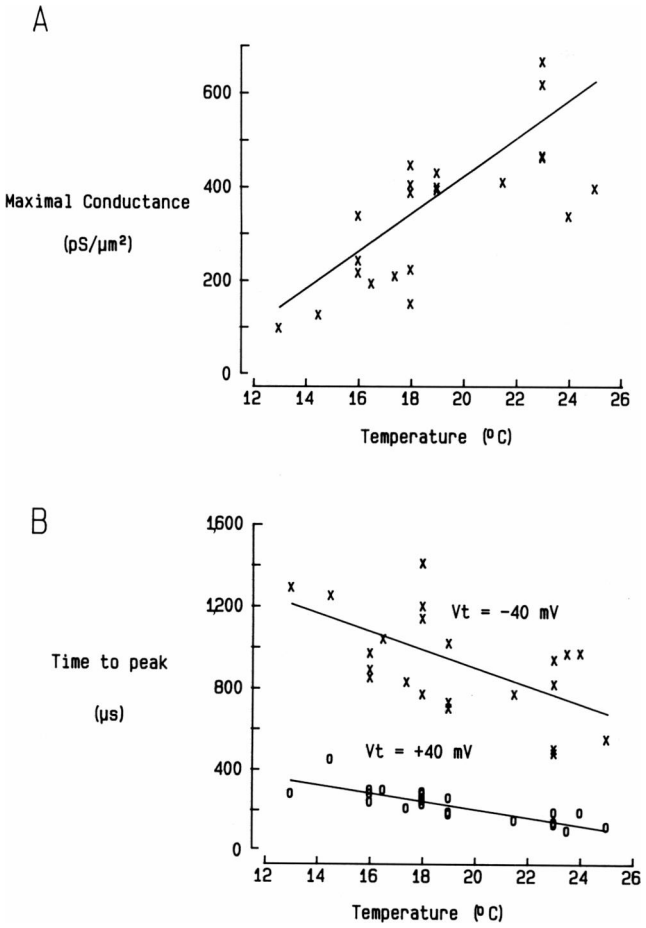

FIGURE 8 (*A*) Temperature dependence of maximal conductance (×, $r = 0.74$) calculated from the positive slope of the peak IV plot (see Fig. 7 *C*). (*B*) Temperature dependence of time to peak I_{Na} for depolarizations to −40 mV (×, $r = 0.57$) and to +40 mV (0, $r = 0.87$) from $V_h = -150$ mV. Values are from 22 different cells studied in standard solutions at the temperatures indicated. Lines represent least squares linear fit with correlation coefficient given by r.

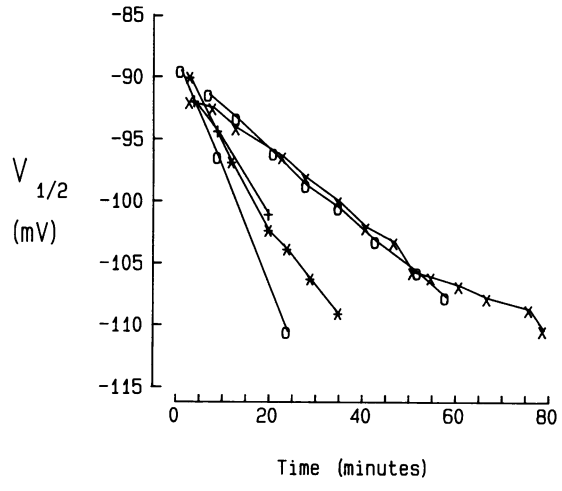

FIGURE 9 Shift in half I_{Na} availability with time in standard solutions for five cells. $V_{1/2}$ is the midpoint of the dependence of peak I_{Na} upon a 500-ms conditioning pulse to V_m as in Fig. 6.

the pipette, the favorable geometry of the Purkinje cell, the study of only a portion of the cell, and the high conductivity of the solutions used.

Control of the Chemical Gradient

The experimental technique allows control of the transmembrane ion gradients by fixing both the internal and external concentrations of the ion of interest and by eliminating interfering ions. $[Na^+]_i$ could be changed within minutes, and $[Na^+]_o$ within seconds, as demonstrated by the close agreement of experimental reversal potentials with those predicted by the Nernst relation.

I_{Na} Characteristics

The sigmoid onset and multiexponential decay of I_{Na} demonstrated here in Purkinje cells resembles previous descriptions of I_{Na} in both nerve and heart, although peak I_{Na} was reached more quickly than previous reports in heart at similar temperatures (Table II). The Hodgkin–Huxley (1952) model assumed no overlap in the time course of activation and inactivation, and predicted the decay of I_{Na} to be a single exponential due entirely to inactivation. Deviation from a single exponential was first noted by Frankenhaeuser (1963) in nodes of Ranvier and has been reported in heart by Brown et al. (1981), Kunze et al. (1985), Patlak and Ortiz (1985), Makielski et al. (1985), and the present study (Fig. 5). Multiexponential decays have been modeled as two populations of channels (Meves, 1978) or as two inactivated states (Chiu, 1977). An alternative explanation is that some I_{Na} channels open for the first time after peak I_{Na} (Aldrich et al., 1983; Horn and Vandenberg, 1984). Single channel studies in rat ventricle (Kunze et al., 1985) and in dog heart Purkinje cells (Scanley et al., 1985) suggest that channel reopenings after peak I_{Na} affect macroscopic decay. The dependence of total charge transfer during I_{Na} on voltage (Fig. 10, discussed below) supports a major role for reopenings in I_{Na} decay.

Patlak and Ortiz (1985) in their patch clamp study of rat ventricular cells showed a dependence of I_{Na} decay upon the holding potential; I_{Na} decay at a test potential of −40 mV had a slower time course when the holding membrane potential was −100 mV than when the holding potential was −150 mV. In contrast, the Purkinje cell has two time constants of decay over a full range of test voltages (Fig. 5) that were not significantly different when holding potential was changed from −150 to −100 mV.

Peak IV Relationship

I_{Na} density in Purkinje cells is greater than previous reports in ventricular and atrial cells (Table II), and differences in study conditions affecting I_{Na} magnitude are unlikely to account for this increased density. I_{Na} increases as the Na gradient increases but the exact relationship between the Na gradient and I_{Na} depends upon the extent of Na^+

TABLE II
I_{Na} IN SINGLE HEART CELLS

	Present study	Brown, 1981	Bodewei, 1981	Bustamante, 1982	Cachelin, 1983	Kunze, 1985	Benndorf, 1985
Cell type	Purkinje dog	Ventricular rat	Ventricular rat	Atrial human	Ventricular rat neonate	Ventricular rat neonate	Ventricular mouse
Pipette	Large glass	Two glass	Large PE	Large PE	Patch	Patch	Large patch
C_m (pF)/SA (μm^2)	65/–	200/8,000	100/4,000	48/1,600	3/314	3/314	186/–
τ_c (μs)/R_s (kΩ)	4.5/70	80/400	40/200				35/192
Temperature (°C)	18	20–22	"Room"	20–22	16–18	20–22	21–23
$[Na^+]_o/[Na^+]_i$ (mM)	45:15	72.5:16	140:0	150:10	147:66*	40:10	52.5:13
$[Ca^{++}]_o$,$[Mg^{++}]_o$ (mM)	3.0, 1.0	0, 2.55	0, 1.2	1.0, 1.0	0.02, 2.0	0.02, 2.0	0, 1.2
Other divalents		Mn	Cd	Mn			
Peak I_{Na} (nA)	200	65	10	15	0.3	1.0	35
at V_t (mV)	at −30	at −26	at −30	at −30	at −15	at −35	at −30
Peak I_{Na} (mA/μF)	2.3	0.4	0.1	0.8	0.1	0.3	.18
G_{Na} (pS/μm^2)	440	49	6.4	42	28	52	31
P_{Na} (cm-s 10^{-5})	41	3.4		10.3	.70	4.5	2.3
Time to peak I_{Na} (ms) at V_t (mV)	0.5 at −30	0.5 at −26	1.5 at −30	0.8 at −30	1.5 at −15	1.3 at −35	0.8 at −30
$V_{1/2}$ (mV)	−94	−70	−78	−75	−70	−85	−76

SA, Surface area of outer membrane (ignoring folding and t-tubules). PE, polyethylene tubing. $V_{1/2}$, conditioning potential that reduces I_{Na} by one-half. V_t, test potential. All other symbols and abbreviations are defined in the text. The values in the table were either reported by the original investigators or were calculated from figures in their studies. Normalization to SA was performed using C_m, or C_m was calculated from cell dimensions assuming 1 $\mu F/cm^2$ and folding factors from the literature. For rat ventricular cells a whole cell C_m = 200 pF (Brown et al., 1980) was used, and it was assumed Bodewei studied one-half of the cell. For human atrial cells C_m was calculated assuming 10% of 16,000 μm^2 (Bustamante et al., 1982) membrane was studied, and assuming a C_m/SA ratio of 3. For rat neonatal cells C_m was calculated from the diameter (10 μm) ignoring folding. This last assumption may overestimate I_{Na} density.
*Estimated from reversal potential.

interaction with the channel (Begenisich and Cahalan, 1980; Sheets et al., 1987). The GHK constant field equation takes into account different Na gradients, but assumes ionic independence, and does not account for saturation. However, the effects of saturation are unlikely to cause large errors in comparing P_{Na} for the concentration ranges in the different studies, and when P_{Na} was calculated for all of the studies, it was greater by an order of magnitude in the present study than in previous studies (Table II). Differences in Na^+ gradient, Ca^{++} concentration, and temperature between this study and the others all tend to favor reduced peak I_{Na} in this study.

Differences in I_{Na} magnitude could be caused by normalization procedures. Surface folding in different cell types can complicate estimation of membrane area from cell dimensions. To allow comparison, the values in Table II have been normalized to measured C_m where possible and to estimated C_m assuming cell dimensions and folding factors if necessary. Na^+ channels may not exist in all surface membrane measured by C_m in single Purkinje cells. Transverse membrane (membrane at the ends of cells) contributes relatively more to C_m because it has greater folding than the remaining membrane (Page and McCallister, 1973). Although gap junctions and their remnants appear to be internalized (Mazet et al., 1985) in the transverse membrane of single cells, the existence and fate of Na^+ channels in this membrane is unknown. Therefore, normalization to C_m may underestimate I_{Na} density, especially in our preparation, where the use of cell fragments of less than one-half the cell length increases the relative contribution of the transverse membrane to total membrane.

Heavy metal ions used in some previous studies (Table II) may have decreased peak I_{Na} as has been demonstrated in nerve (Århem, 1980). In our experience Mn^{++} reduced I_{Na} and 1.0 mM Cd^{++} completely blocked I_{Na} (unpublished observations; see also DiFrancesco et al., 1985; Frelin et al., 1986). The use of Cd^{++} by Bodewei et al. (1982) and the use of Mn^{++} by Brown et al. (1981) and Bustamante and McDonald (1983) likely contributed to the reduced I_{Na} seen in their studies. Here Ca^{++} channel blockers were not used because studies with TTX showed that the contamination of I_{Na} by Ca^{++} current was negligible. In all studies that use heavy metals as Ca^{++} channel blockers their possible effects on I_{Na} must be considered.

I_{Na} Channel Density

The high current density we observed in single Purkinje cells implies a high Na^+ channel density. Patch clamp studies on Purkinje cells in this laboratory gave single channel conductance (γ_{Na}) of 11 pS in 140 mM $[Na^+]_o$ at 13°C (Scanley et al., 1985), which is comparable to γ_{Na} in other studies in heart (Grant et al., 1983; Kunze et al.,

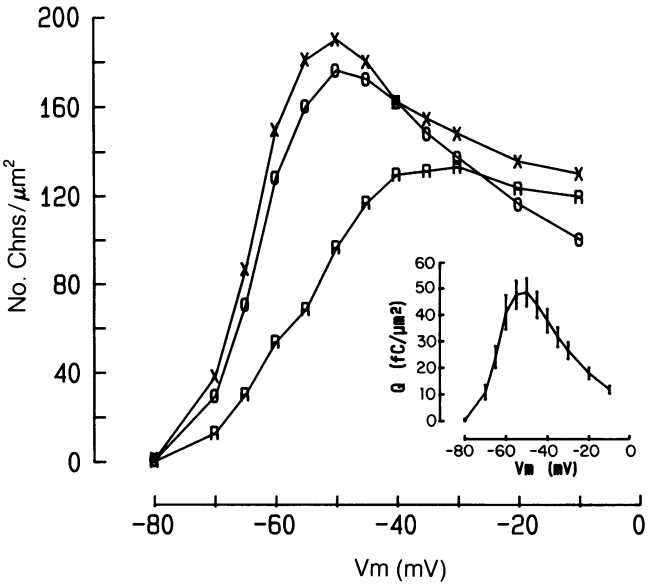

FIGURE 10 Voltage dependence of channel openings during step depolarizations. Channel openings were measured by integrating I_{Na} at each potential and dividing by the charge transferred per channel opening. The number of openings were computed for the potentials indicated by assuming a constant mean open time of 0.7 ms (0), a dependence of mean open time on voltage with mean open time first increasing then decreasing with stronger depolarizations (×), and a dependence of mean open time on voltage and also a dependence of channel reopenings on voltage (*R*). Note that correcting for reopenings makes the curve relatively flat for potentials > −30 mV. Data are means of eight cells in 45 mM $[Na^+]_o$, 15 mM $[Na^+]_i$, 18°C. The inset shows the voltage dependence of total charge transfer (± SE) during a depolarization from the same eight cells.

1985). This γ_{Na}, corrected for different Na^+ gradients and temperature, was used to calculate channel density from peak I_{Na} measurements and slope conductance. The mean for eight different cells with 45 mM $[Na^+]_o$ was 67 ± 17 channels/μm^2 open at peak I_{Na} (−40 mV).

The number of Na^+ channels open at peak I_{Na} necessarily underestimates the total number of Na^+ channels in the membrane because some channels inactivate before peak current, others inactivate without opening, and others first activate after peak current. To better estimate channel density we integrated I_{Na} in the eight cells studied in 45:15 $[Na^+]_o/[Na^+]_i$ at 18°C to give the charge transferred during step depolarizations (Fig. 10, *inset*), and divided by mean charge transferred per channel opening at each potential, which was obtained from single channel current measurements (Scanley et al., 1985) multiplied by mean open time. Using a constant mean open time of 0.7 ms at 18°C (Nagy et al., 1983), estimates of channel openings during depolarization increase between −80 and −50 mV (Fig. 10, *circles*) as the result of increasing activation (Fig. 6), and then decline with more positive depolarization. A similar decline was observed by Bean (1981) in crayfish axons, and he suggested that it was caused by a voltage dependence of inactivation from the open state. Patch clamp studies have reported a weak (Nagy et al., 1983) or negligible (Aldrich et al., 1983) decline of mean open time positive to −40 mV. In cardiac Purkinje cells mean open time has a biphasic dependence upon voltage (Scanley, 1987) that is similar to the voltage dependence reported for GH_3 cells (Horn and Vandenberg, 1984). Correction for the Purkinje cell dependence of mean open time on voltage shows that it explains only a small part of the decline (Fig. 10, *crosses*).

Channel reopenings during depolarization would cause that channel to be counted twice. Reopenings appear to be common in cardiac tissue (Kunze et al., 1985; Scanley et al., 1985) and show a sigmoidal voltage dependence such that increasingly positive depolarizations diminish the probability of reopening (Scanley, 1987). Correcting for reopenings at each test voltage can account for most of the declining portion of the channel opening–voltage relationship (Fig. 10, *R*); 130 ± 15 channels/μm^2 open during depolarizations positive to −45 mV. This is an underestimate of the total channel density because some channels inactivate without opening. Null sweeps, sweeps during a patch clamp depolarization in which no openings are observed, give a measure of how often this occurs, and a reasonable estimate of the percentage of null sweeps at −40 mV is 50% or greater (Aldrich et al., 1983; Scanley et al., 1985). Thus, the best estimate of the density of Na^+ channels in the cardiac Purkinje cell membrane is 260 channels/μm^2. This can be compared with channel densities of 1.5–10 channels/μm^2 in chromaffin cells (Fenwick et al., 1982), 330 channels/μm^2 in squid axons (Conti et al., 1975), and 1,900 channels/μm^2 in frog node (Sigworth, 1980). The channel density estimate of 5 channels/μm^2 from previous studies in atrial and ventricular tissue (Fozzard et al., 1985) is far less than our results. Although experimental conditions in previous studies may have led to an underestimate of channel density, we suspect there may be a greater channel density in the specialized conducting tissue of the heart.

Hyperpolarizing Shift

Na^+ channel availability (Fig. 6) measured in these experiments by peak I_{Na} had a more negative dependence upon voltage than estimates from experiments using maximal upstroke velocity in Purkinje fibers (Weidmann, 1955) and Purkinje cells (Sheets et al., 1983). This difference between I_{Na} and maximal upstroke velocity experiments was predicted, at least in part, by Strichartz and Cohen (1978) and has been observed in Purkinje fibers (Cohen et al., 1984) and Purkinje cells (Fozzard et al., 1987). However, the time-dependent negative voltage shift of kinetic parameters noted by us and by others (Sachs and Specht, 1981; Fenwick et al., 1982; Cachelin et al., 1983; Fernandez et al., 1984; Kunze et al., 1985) remains unexplained. Furthermore, our shift appears to be larger and occurs more quickly than that reported by some investigators in other preparations, perhaps because our

use of a large bore suction pipette leads to more rapid and complete washout of some important intracellular component. Fernandez et al. (1984) showed in the GH_3 pituitary cell line that the negative shift occurred for tetraphenylborate displacement currents as well as for I_{Na}, implying that the shift is caused by changes in surface potential rather than a specific change in the Na^+ channel.

The authors thank A. I. Undrovinas of the All Union Cardiology Research Center USSR for early help in voltage clamping single cells and G. J. Sawicki for technical assistance.

This work was supported by National Institutes of Health grants 2-PO1-HL-20692-10, 1-K11-HL01572-01, 1-K11-HL01447, and T-32-HL07381.

Received for publication 1 May 1986 and in final form 13 February 1987.

REFERENCES

Aldrich, R. W., D. P. Corey, and C. F. Stevens. 1983. A reinterpretation of mammalian sodium channel gating based on single channel recording. *Nature (Lond.).* 306:436–441.

Århem, P. 1980. Effects of some heavy metal ions in the ionic currents of myelinated fibres from *Xenopus laevis*. *J. Physiol. (Lond.).* 306:210–231.

Bean, B. 1981. Sodium channel inactivation in the crayfish giant axon: must channels open before inactivating? *Biophys. J.* 35:595–614.

Beeler, G. W., and J. A. S. McGuigan. 1978. Voltage clamping of multicellular myocardial preparations: capabilities and limitations of existing methods. *Prog. Biophys. Mol. Biol.* 34:219–254.

Begenisich, T. B., and M. D. Cahalan. 1980. Sodium channel permeation in squid axons. II. Non-independence and current voltage relations. *J. Physiol. (Lond.).* 307:243–257.

Benndorf, K., W. Boldt, and B. Nilius. 1985. Sodium current in single myocardial mouse cells. *Pfluegers Arch. Eur. J. Physiol.* 404:190–196.

Bodewei, R., S. Hering, B. Lemke, L. V. Rosenshtraukh, A. I. Undrovinas, and A. Wollenberger. 1982. Characterization of the fast sodium current in isolated rat myocardial cells: simulation of the clamped membrane potential. *J. Physiol. (Lond.).* 325:301–315.

Brown, A. M., K. S. Lee, and T. Powell. 1981. Sodium currents in single rat heart muscle cells. *J. Physiol. (Lond.).* 318:479–500.

Brown, A. M., K. Morimoto, Y. Tsuda, and D. L. Wilson. 1980. Calcium current-dependent and voltage-dependent inactivation of calcium channels in *Helix aspersa*. *J. Physiol. (Lond.).* 320:193–218.

Bustamante, J. O., and T. F. McDonald. 1983. Sodium currents in segments of human heart cells. *Science (Wash. DC).* 220:320–321.

Bustamante, J. O., T. Watanabe, D. A. Murphy, and T. F. McDonald. 1982. Isolation of single atrial and ventricular cells from the human heart. *Can. Med. Assoc. J.* 126:791–793.

Cachelin, A. B., J. E. de Peyer, S. Kokubun, and H. Reuter. 1983. Sodium channels in cultured cardiac cells. *J. Physiol. (Lond.).* 340:389–402.

Chiu, S. Y. 1977. Inactivation of sodium channels: second order kinetics in myelinated nerve. *J. Physiol. (Lond.).* 273:573–596.

Cohen, C. J., B. P. Bean, and R. W. Tsien. 1984. Maximal upstroke velocity as an index of available sodium conductance. Comparison of maximal voltage clamp measurements of sodium current in rabbit Purkinje fibers. *Circ. Res.* 54:636–651.

Colatsky, T. J. 1980. Voltage clamp measurements of sodium channel properties in rabbit cardiac Purkinje fibers. *J. Physiol. (Lond.).* 305:215–234.

Cole, K. S., and J. W. Moore. 1960. Ionic current measurements in the squid giant axon membrane. *J. Gen. Physiol.* 44:123–167.

Conti, F., L. J. DeFelice, and E. Wanke. 1975. Potassium and sodium ion current noise in the membrane of the squid giant axon. *J. Physiol. (Lond.).* 248:45–82.

DiFrancesco, D., A. Ferroni, M. Mazzanti, and C. Tromba. 1985. Fast Na current inhibition by cations of group 2b in isolated guinea pig and neonatal rat cardiac cells. *J. Physiol. (Lond.).* 369:87P.

Ebihara, L., N. Shigeto, M. Lieberman, and E. A. Johnson. 1980. The initial inward current in spherical clusters of chick embryonic heart cells. *J. Gen. Physiol.* 75:437–456.

Fenwick, E. M., A. Marty, and E. Neher. 1982. Sodium and calcium channels in bovine chromaffin cells. *J. Physiol. (Lond.).* 331:599–635.

Fernandez, J. M., A. P. Fox, and S. Krasne. 1984. Membrane patches and whole cell membranes: a comparison of electrical properties in rat clonal pituitary (GH_3) cells. *J. Physiol. (Lond.).* 356:565–585.

Fozzard, H. A., and G. W. Beeler, Jr. 1975. The voltage clamp and cardiac electrophysiology. *Circ. Res.* 37:403–413.

Fozzard, H. A., C. T. January, and J. C. Makielski. 1985. Brief review: studies of the excitatory sodium currents in heart muscle. *Circ. Res.* 56:475–485.

Fozzard, H. A., D. A. Hanck, J. C. Makielski, and M. F. Sheets. 1986. Shift in inactivation and activation parameters of Na^+ current in internally dialyzed canine cardiac Purkinje cells. *J. Physiol. (Lond.).* 371:194P.

Fozzard, H. A., D. A. Hanck, and M. F. Sheets. 1987. Nonlinear relationship of maximal upstroke velocity to sodium current in single canine cardiac Purkinje cells. *J. Physiol. (Lond.).* 382:104P.

Frankenhaeuser, B. 1963. Inactivation of the sodium-carrying mechanism in myelinated nerve fibres of *Xenopus laevis*. *J. Physiol. (Lond.).* 169:445–451.

Frelin, C., C. Cognard, P. Vigne, and M. Lazdunski. 1986. Tetrodotoxin sensitive and tetrodotoxin resistant Na^+ channels differ in their sensitivity to Cd^{2+} and Zn^{2+}. *Eur. J. Pharmacol.* 122:245–250.

Grant, A. O., C. F. Starmer, and H. C. Strauss. 1983. Unitary sodium channels in isolated cardiac myocytes of rabbit. *Circ. Res.* 53:823–829.

Hodgkin, A. L., and B. Katz. 1949. The effect of sodium ions on the electrical activity of the giant axon of the squid. *J. Physiol. (Lond.).* 108:37–77.

Hodgkin, A. L., and A. F. Huxley. 1952. A quantitative description of membrane current and its application to conduction and excitation in nerve. *J. Physiol. (Lond.).* 117:500–544.

Horn, R., and C. A. Vandenberg. 1984. Statistical properties of single sodium channels. *J. Gen. Physiol.* 84:505–534.

Johnson, E. A., and M. Lieberman. 1971. Heart: excitation and contraction. *Annu. Rev. Physiol.* 33:479–532.

Kostyuk, P. G. 1984. Intracellular perfusion of nerve cells and its effects on membrane currents. *Physiol. Rev.* 64:435–454.

Kunze, D. L., A. E. Lacerda, D. L. Wilson, and A. M. Brown. 1985. Cardiac Na currents and the inactivating, reopening, and waiting properties of single sodium channels. *J. Gen. Physiol.* 86:691–720.

Makielski, J. C., M. F. Sheets, C. T. January, and H. A. Fozzard. 1985. Can sodium current inactivate without first activating in cardiac Purkinje cells? *J. Gen. Physiol.* 86:12a. (Abstr.)

Mathias, R. T., B. R. Eisenberg, N. B. Datyner, G. A. Gintant, and I. S. Cohen. 1985. Impedance and morphology of isolated canine cardiac Purkinje myocytes: comparison with intact strand preparations. *Biophys. J.* 47(2, Pt. 2):499a. (Abstr.)

Mazet, F., B. A. Wittenberg, and D. Spray. 1985. Fate of intercellular junctions in isolated rat cardiac cells. *Circ. Res.* 56:195–204.

Meves, H. 1978. Inactivation of the sodium permeability in squid giant nerve fibres. *Prog. Biophys. Mol. Biol.* 33:207–230.

Nagy, K., T. Kiss, and D. Hof. 1983. Single Na channels in mouse neuroblastoma cell membrane, indication for two open states. *Pfluegers Arch. Eur. J. Physiol.* 399:302–308.

Page, E., and L. P. McCallister. 1973. Studies on the intercalated disk of rat left ventricular cells. *J. Ultrastruct. Res.* 43:388–411.

Patlak, J. B., and M. Ortiz. 1985. Slow currents through single sodium channels of the adult rat heart. *J. Gen. Physiol.* 86:691–720.

Provencher, S. W. 1976. A Fourier method for the analysis of exponential decay curves. *Biophys. J.* 16:27–41.

Rogart, R. 1981. Sodium channels in nerve and muscle membrane. *Annu. Rev. Physiol.* 43:711–725.

Sachs, F., and P. Specht. 1981. Sodium currents in single cardiac Purkinje cells. *Biophys. J.* 33(2, Pt. 2):123a. (Abstr.)

Scanley, B. E., D. Hanck, M. F. Sheets, and H. A. Fozzard. 1985. Reopening behavior of Na channels in isolated canine cardiac Purkinje cells. *J. Gen. Physiol.* 86:12a. (Abstr.)

Scanley, B. E. 1987. Patch clamp study of single sodium channels in canine cardiac Purkinje cells. Ph.D. thesis. University of Chicago, Chicago, IL.

Sheets, M. F., C. T. January, and H. A. Fozzard. 1983. Isolation and characterization of single canine Purkinje cells. *Circ. Res.* 53:544–548.

Sheets, M. F., B. G. Scanley, D. A. Hanck, J. C. Makielski, and H. A. Fozzard. 1987. Open sodium channel properties of single canine cardiac. Purkinje cells. *Biophys. J.* 52:13–22.

Sigworth, F. J. 1980. The conductance of sodium channels under conditions of reduced current at the node of Ranvier. *J. Physiol. (Lond.).* 307:131–142.

Sommer, J. R., and E. A. Johnson. 1979. Ultrastructure of cardiac muscle. *In* Handbook of Physiology. Section 2: The Cardiovascular System. Vol. I: The Heart. R. M. Berne and N. Sperelakis, editors. Am. Physiol. Soc., Bethesda. 113–186.

Strichartz, G., and I. Cohen. 1978. $\dot{V}_{max}$ as a measure of $\overline{G_{Na}}$ in nerve and cardiac membranes. *Biophys. J.* 23:153–156.

Weidmann, S. 1955. The effect of the cardiac membrane potential on the rapid availability of the sodium-carrying system. *J. Physiol. (Lond.).* 127:213–224.